NIF Polar-Drive High DT-Yield Exploder-Pusher Designs Modeled Using Pump Depletion in *DRACO*

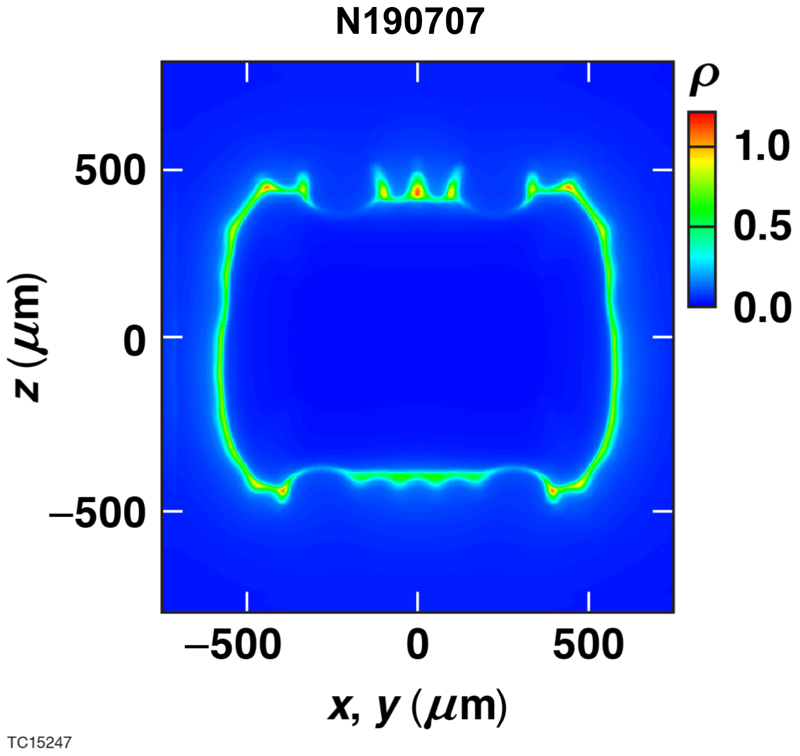

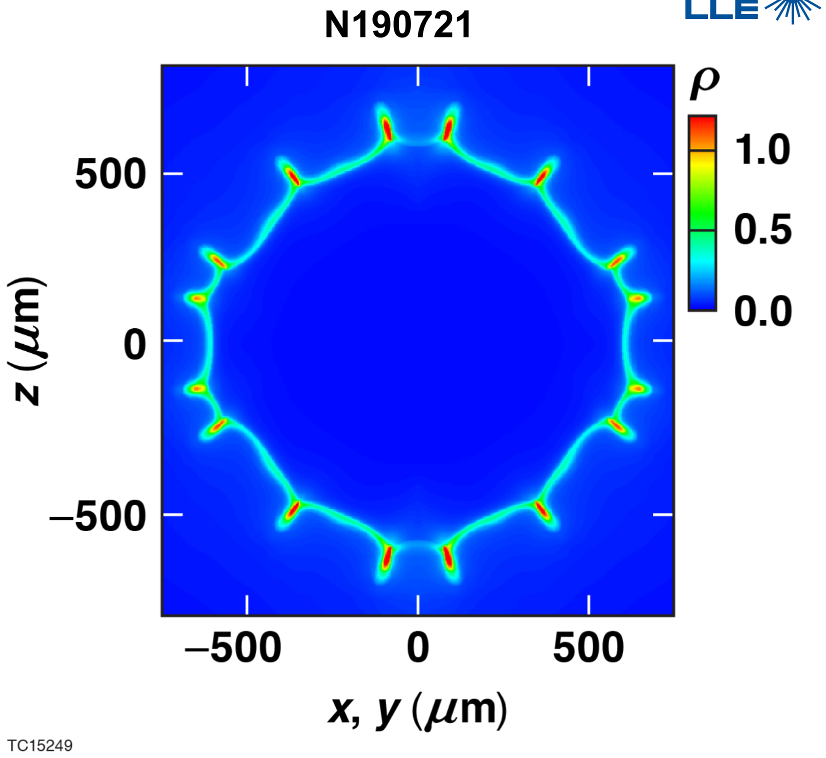

J. A. Marozas
University of Rochester
Laboratory for Laser Energetics

61st Annual Meeting of the
APS Division of Plasma Physics
Fort Lauderdale, FL
21–25 October 2019

NIF Polar-Drive High DT-Yield Exploder-Pusher Designs Modeled Using Pump Depletion in *DRACO*

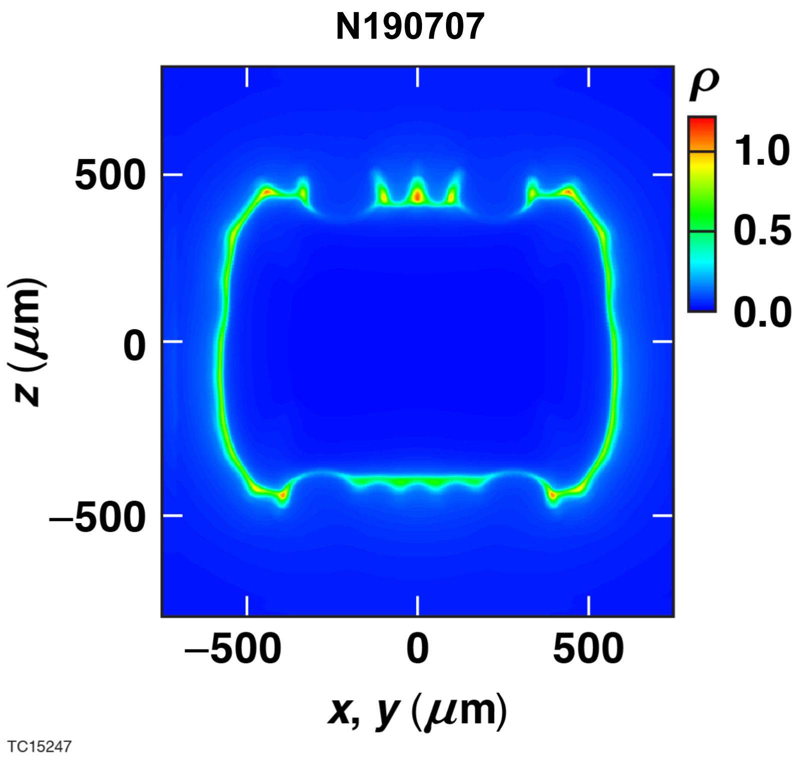

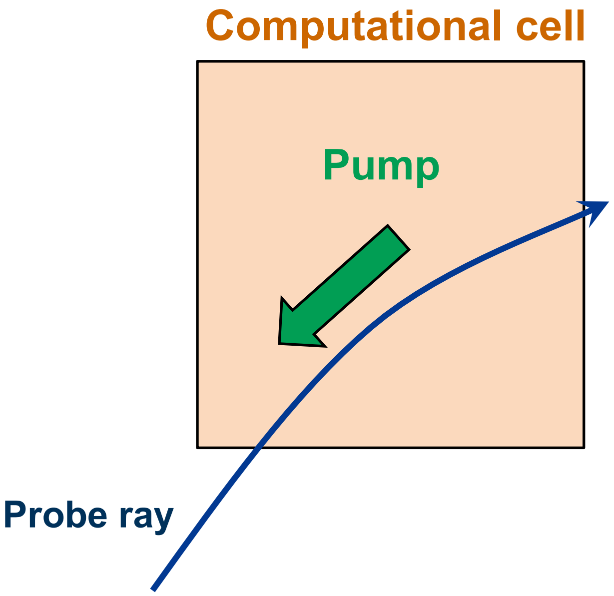

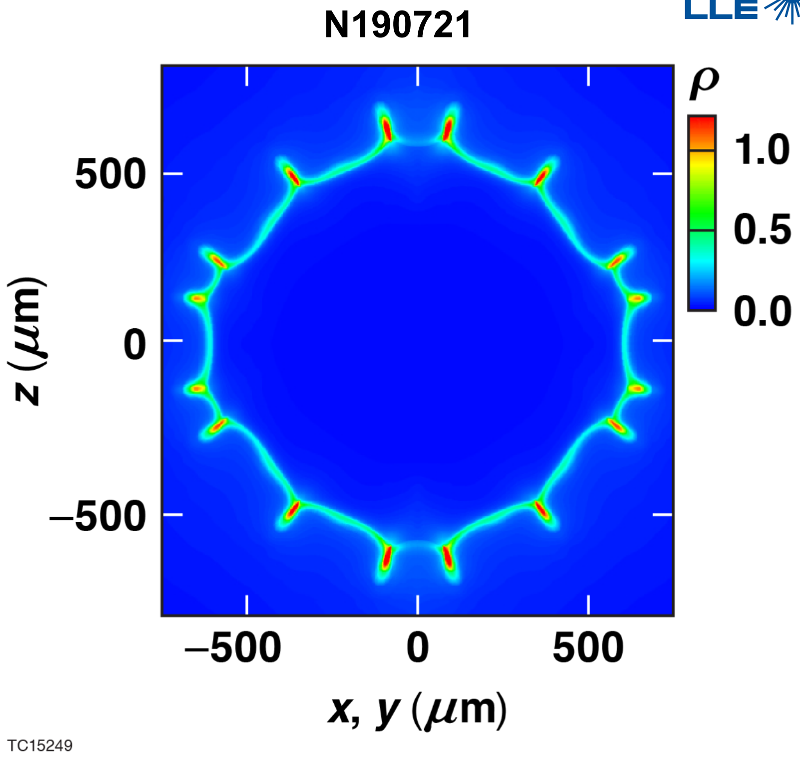

J. A. Marozas
University of Rochester
Laboratory for Laser Energetics

61st Annual Meeting of the
APS Division of Plasma Physics
Fort Lauderdale, FL
21–25 October 2019

NIF Polar-Drive High DT-Yield Exploder-Pusher Designs Modeled Using Pump Depletion in *DRACO*

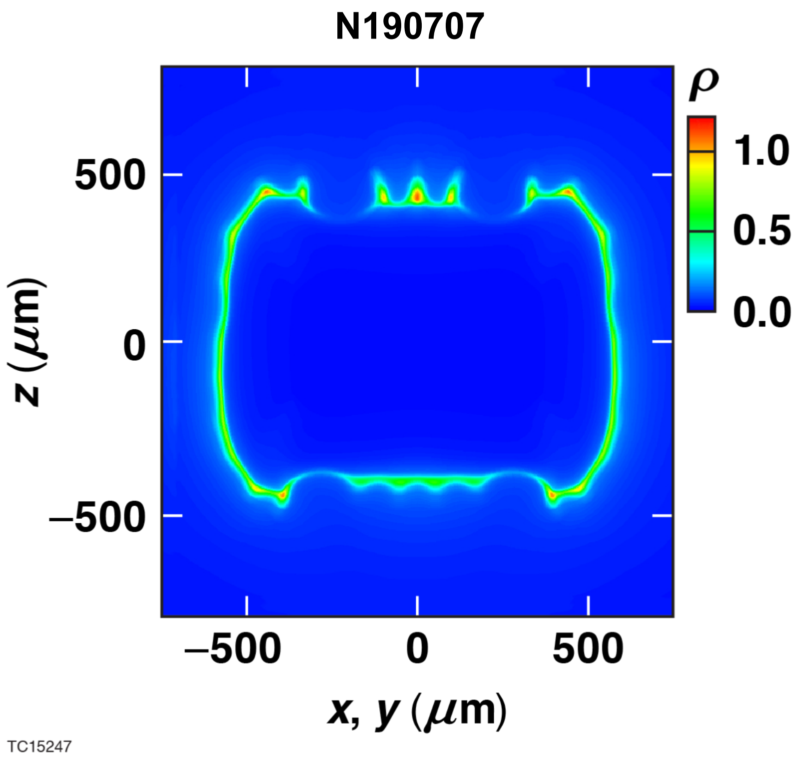

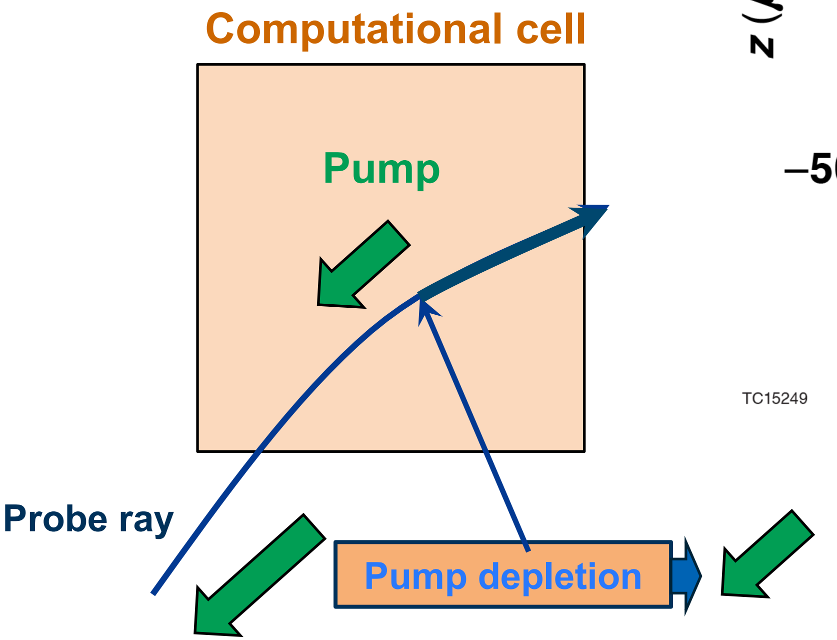

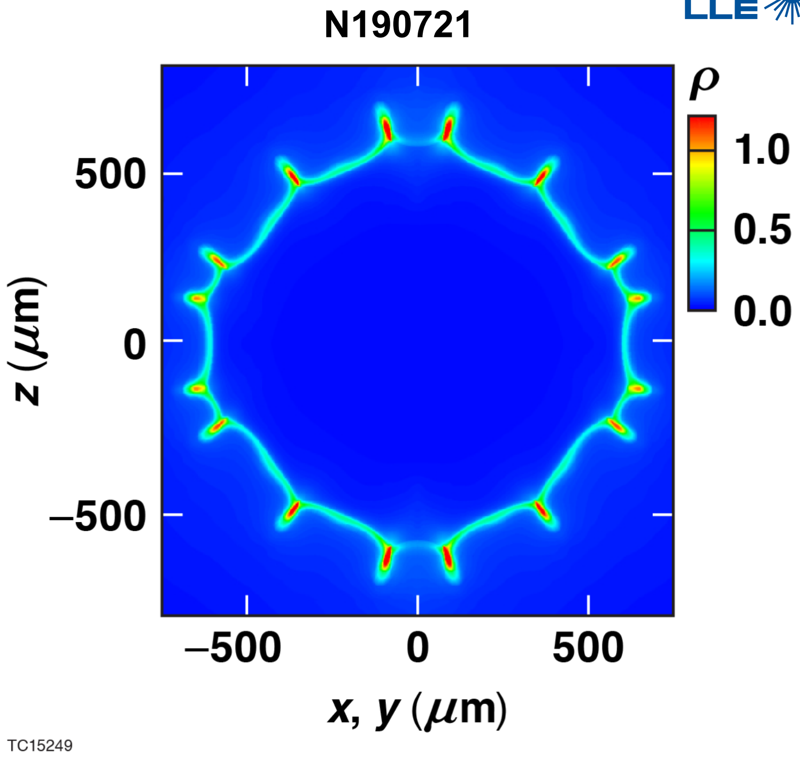

J. A. Marozas
University of Rochester
Laboratory for Laser Energetics

61st Annual Meeting of the
APS Division of Plasma Physics
Fort Lauderdale, FL
21–25 October 2019

Summary

Exploding pusher (XP) designs using *DRACO* with pump depletion provide a pathway to higher yields while forming a platform to study laser-energy coupling

- Recent NIF XP shots in polar direct drive (PDD) induce unbounded cross-beam energy (CBET) gain given the infinite source-term of the Randall formulation*
- Pump depletion naturally limits CBET gain by reducing the pump-field magnitude and converges to a physically realistic solution without *ad hoc* multipliers
  - applicable to both low- and high-intensity implosions**
- The CBET modeling with pump depletion facilitates predictive simulations

* C. J. Randall, J. R. Albritton, and J. J. Thomson, Phys. Fluids 24, 1474 (1981).
** P. W. McKenty *et al.*, YO6.00006, this conference.
K. Anderson *et al.*, NO5.00009, this conference.
NIF: National Ignition Facility

Collaborators

**P. W. McKenty, T. J. B. Collins, M. J. Rosenberg, P. B. Radha,
S. P. Regan, S. Miller, and E. M. Campbell**

University of Rochester, Laboratory for Laser Energetics

**C. B. Yeamans, B. Blue, L. Divol, W. W. Hsing,
G. E. Kemp, and H. D. Whitley**

Lawrence Livermore National Laboratory

Recent NIF PDD-XP experiments provide high-yield neutron sources that challenge prior simulation capabilities

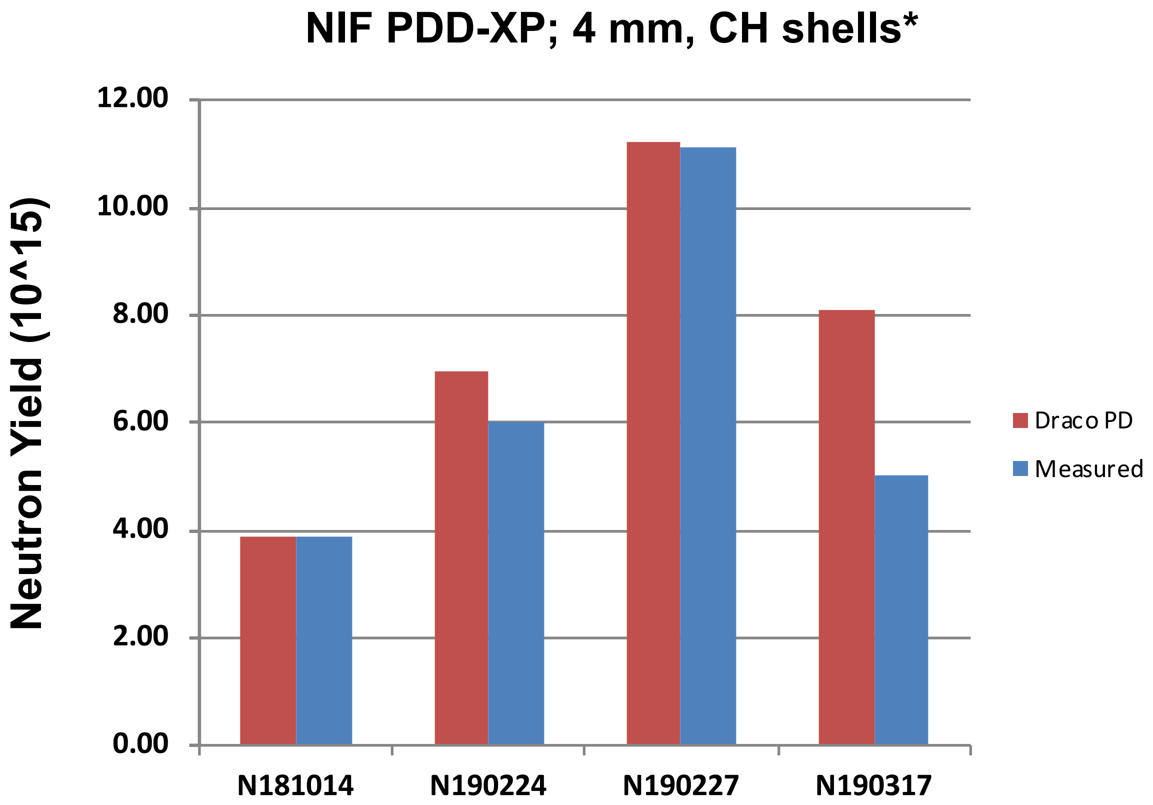

- Excessive CBET gain of the PDD-XP previously prevented converged simulations
- CBET with pump depletion naturally controls the gain
  - results in a predictive capability without any *ad hoc* multipliers
- Lower-intensity OMEGA simulations have also benefited from CBET with pump depletion**

XP simulations require CBET with pump depletion because of their higher intensity and faster implosion speeds.

* P. W. McKenty *et al.*, YO6.00006, this conference.
** K. Anderson *et al.*, NO5.00009, this conference.

The CBET model in *DRACO* now includes pump depletion, which eliminates any need for an arbitrary prefactor and improves predictability

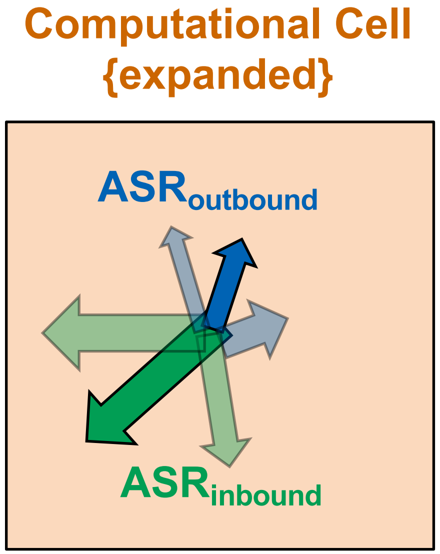

- **The star-shaped angular-spectrum representation (ASR) pump-spectrum prior to interaction with a probe ray**

The CBET model in *DRACO* now includes pump depletion, which eliminates any need for an arbitrary prefactor and improves predictability

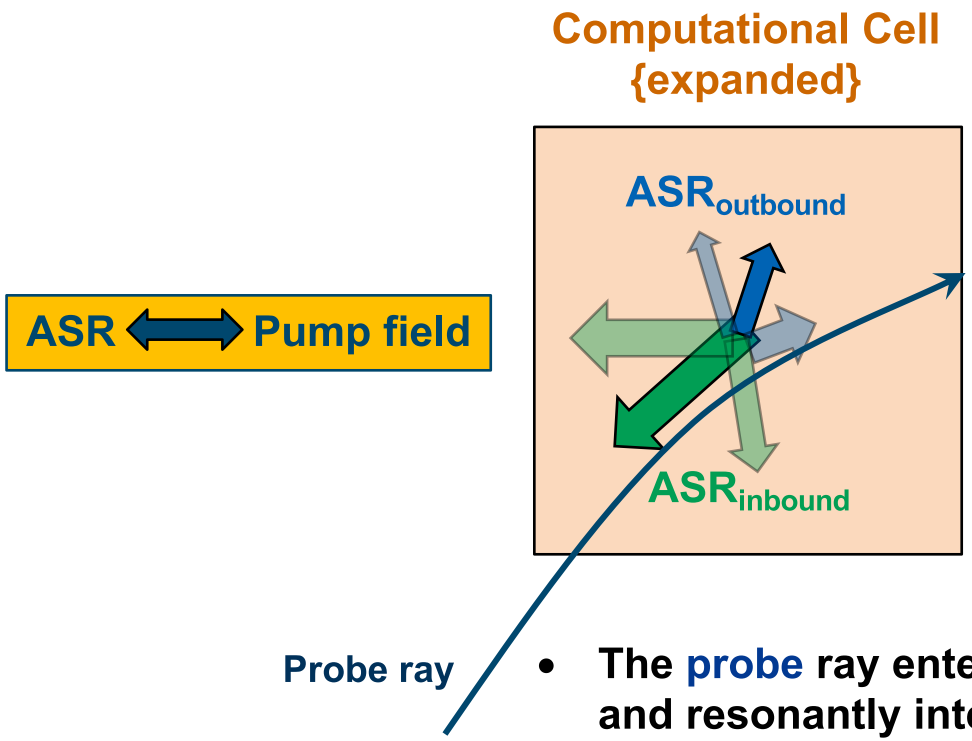

- The **probe** ray enters the computational-cell and resonantly interacts with one component of the $ASR_{inbound}$

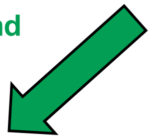

The CBET model in *DRACO* now includes pump depletion, which eliminates any need for an arbitrary prefactor and improves predictability

ASR ⟺ Pump field

Computational Cell
{expanded}

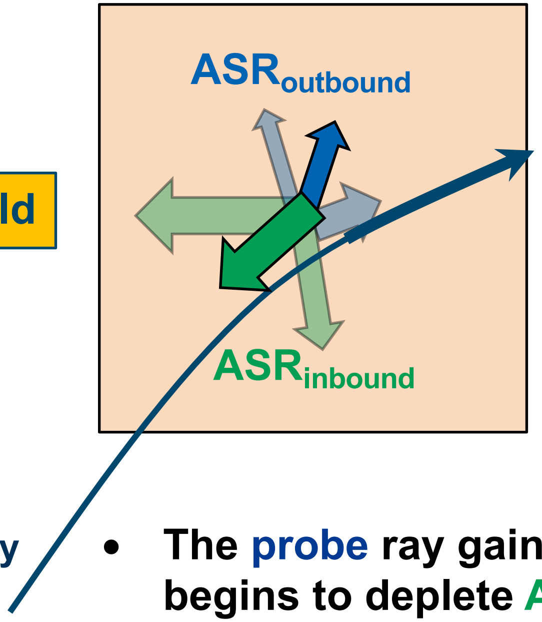

Probe ray

- The probe ray gains significant energy and begins to deplete $ASR_{inbound}$

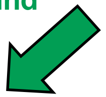

- The ASR now has less intensity to contribute to subsequent rays

The CBET model in *DRACO* now includes pump depletion, which eliminates any need for an arbitrary prefactor and improves predictability

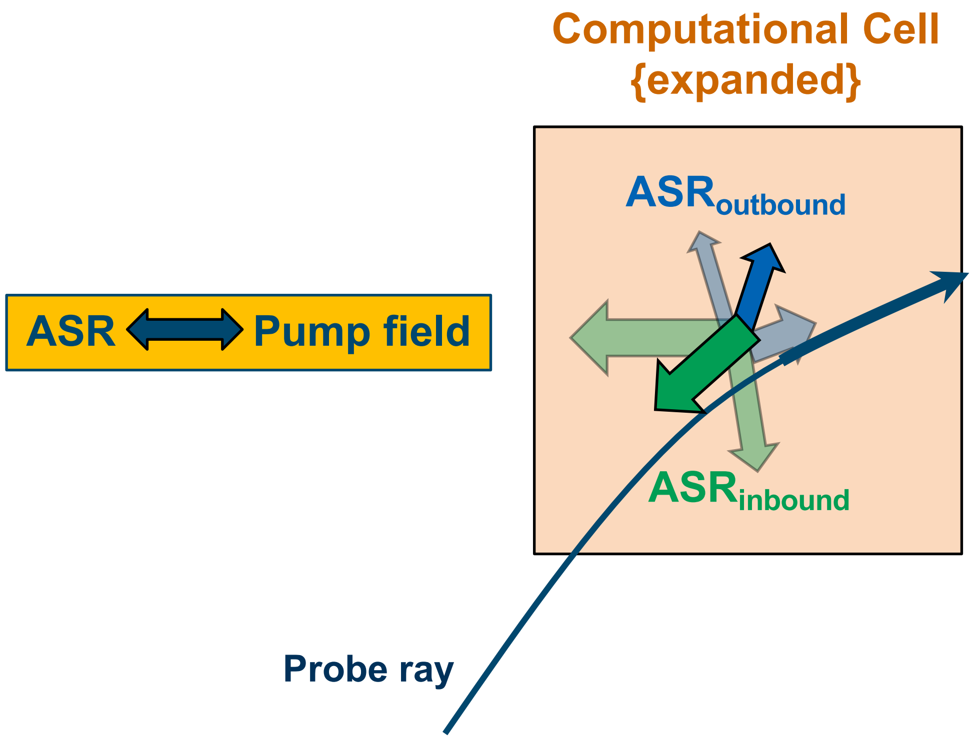

- CBET pump depletion modeling physically limits unbounded growth, naturally controlling CBET gain
  - eliminates the need for an arbitrary CBET prefactor
  - achieves energy balance and conservation without unphysical saturation or unphysical boost compensation used in other codes
  - as a result, *DRACO* has greater predictive capabilities

A post-shot simulation of N190707 models the relevant physics and closely predicts the experimental DT yield (4.8×10^{15})

N190707-001 3 mm, 18 μm CH, 8 atm DT (65/35), $\Delta\lambda_0 = \{9.7, 8.5, 1.2\}$Å, IR

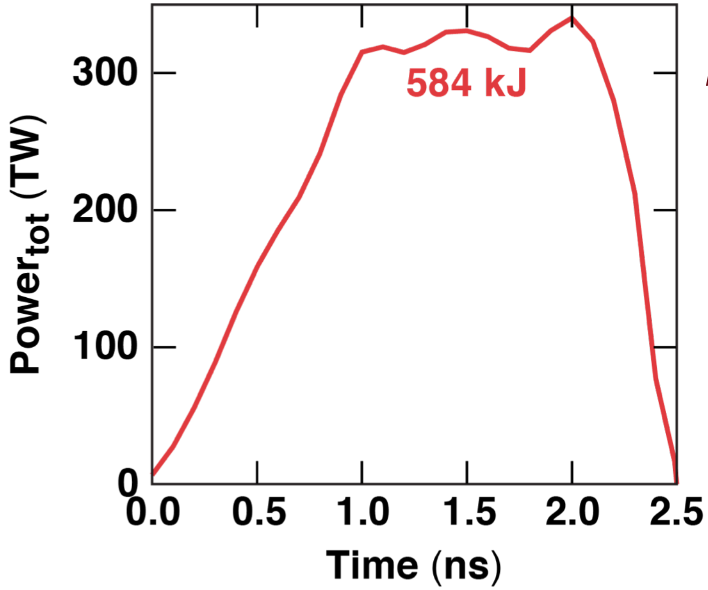

TC15245

DRACO: $Y_{DT} = 4.94 \times 10^{15}$
T_i = 12.0 keV
t_{bang} = 2.84 ns
t_{burn} = 202 ps

Exp: $Y_{DT} = 4.81 \times 10^{15}$
T_i = 11.1 keV
t_{bang} = 2.71 ns
t_{burn} = 311 ps

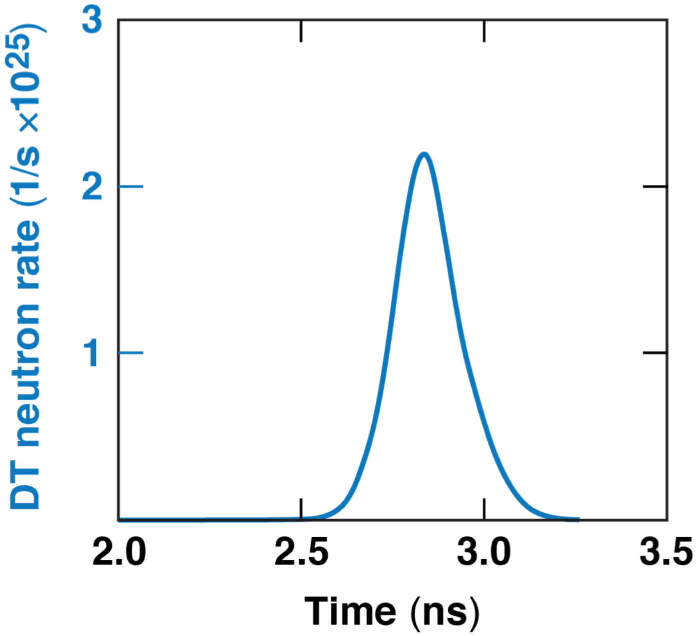

TC15246

These smaller 3-mm targets have low laser impact.

A new pointing pulse-shaping and dual-shock approach was attempted that promises to extend XP yields into the 100-kJ range

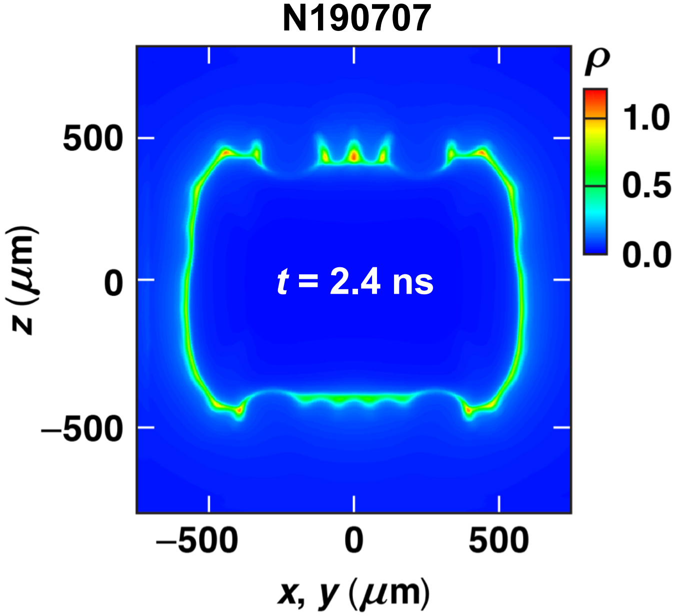

TC15247

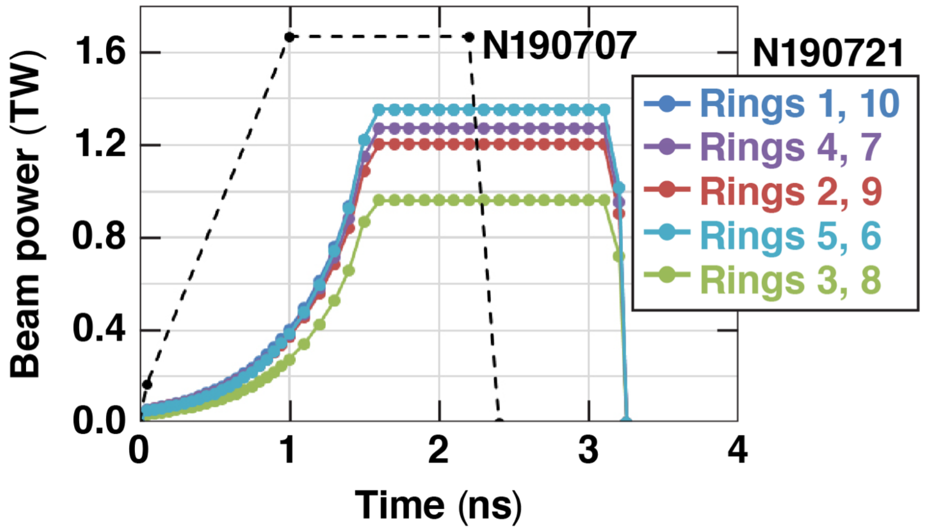

TC15248

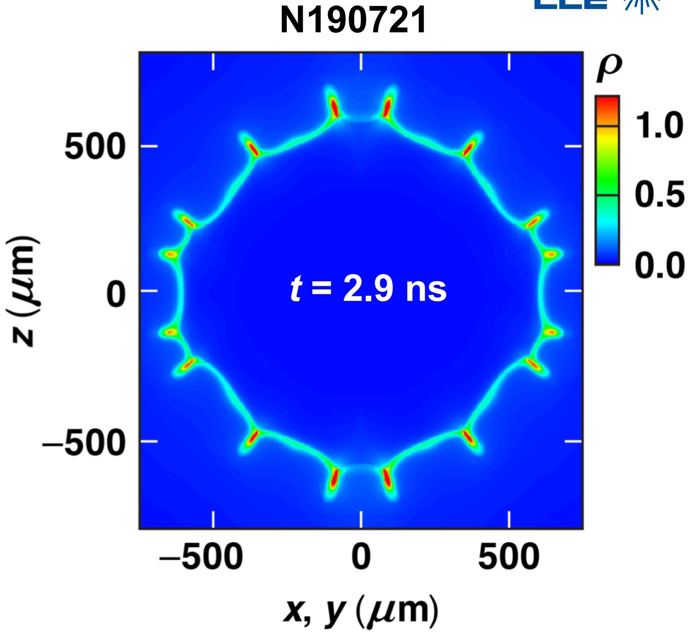

TC15249

- Dual shocks improve yield
- The pulse shape improves separation of shell from shock, improving yield
- Steep main-pulse rise improves coupling
- Simpler quad-splitting improves power imbalance
- Repointing and pulse shapes yield rounder implosions

A pre-shot simulation of N190721 models the relevant physics; however, predicted yields were higher than the experimental DT yield (2.45 × 10^15)

N190721-001 3 mm, 18 μm CH, 6 atm DT (65/35), $\Delta\lambda_0 = \{9.7, 8.5, 1.2\}$Å, IR

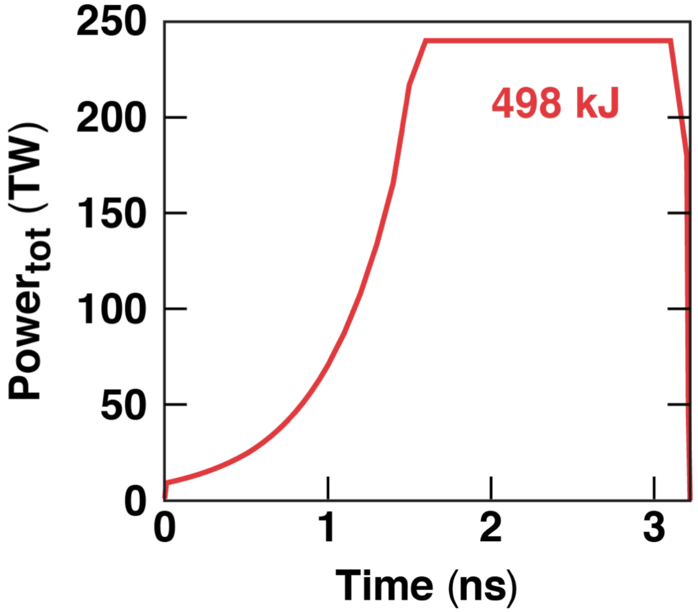

TC15250

***DRACO*: preShot** Y_{DT} = 6.99 × 10^{15}
T_i = 12.8 keV
t_{bang} = 3.43 ns
t_{burn} = 207 ps

Exp: Y_{DT} = 2.45 × 10^{15}
T_i = 10.4 keV
t_{bang} = 3.5 ns
t_{burn} = 319 ps

Hypothesis: The fill pressure was too low, poor power-balance or second shock was mistimed.

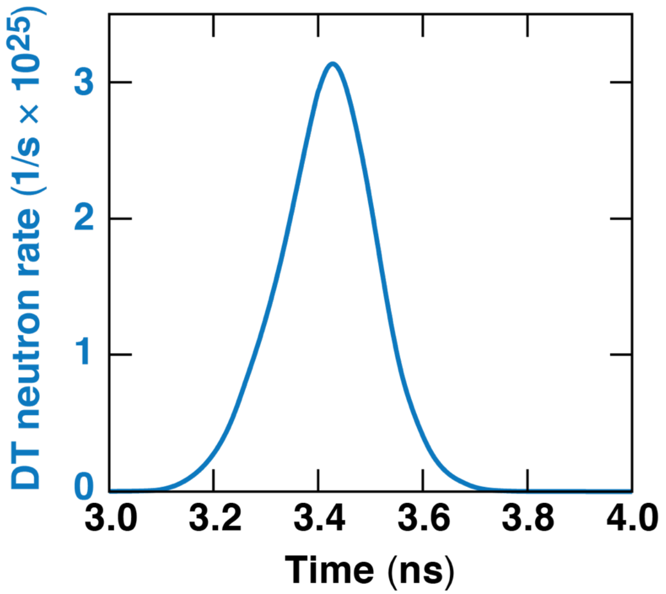

TC15251

A post-shot simulation of N190721 reveals the significant effect of power balance that can be remedied via learning from the pulse-shape at low power-levels

N190721-001 3 mm, 18 μm CH, 6 atm DT (65/35), $\Delta\lambda_0 = \{9.7, 8.5, 1.2\}$Å, IR

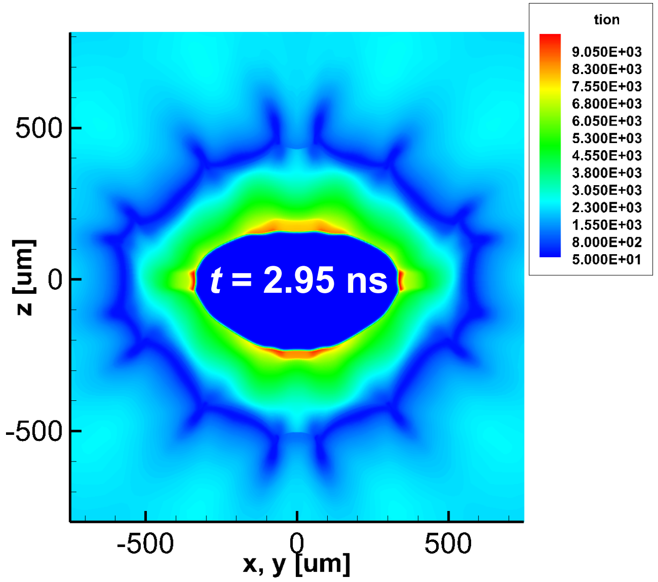

Early time power-balance caused significant oblate shell and flattened Northern-hemi L==1.

Experimental equatorial neutron images:**

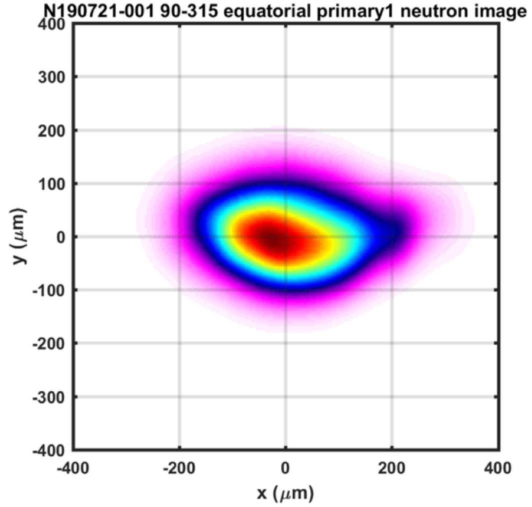

** P. Volegov, Los Alamos National Laboratory, private communication (2019).

Shot N190721 lies on a steep performance curve and further study of equatorial laser coupling should dramatically improve yield

- Previous XP shots showed a steeper experimental yield cliff <6 atm
- Some attributes of N190721 cf. N190707:
  - higher predicted absorption fraction; lower predicted CBET
  - higher experimental convergence ratio—7.3 versus 8.4; even though it used less energy—(585 versus 495 kJ)
  - better azimuthal symmetry

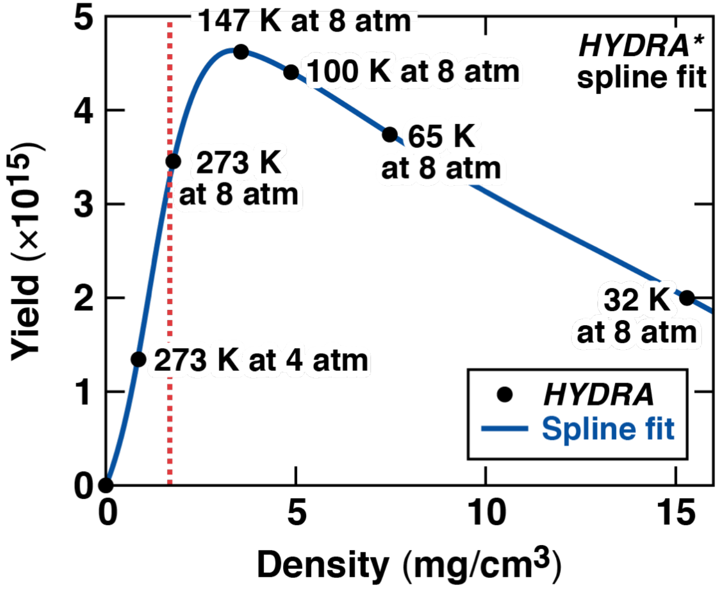

TC15252

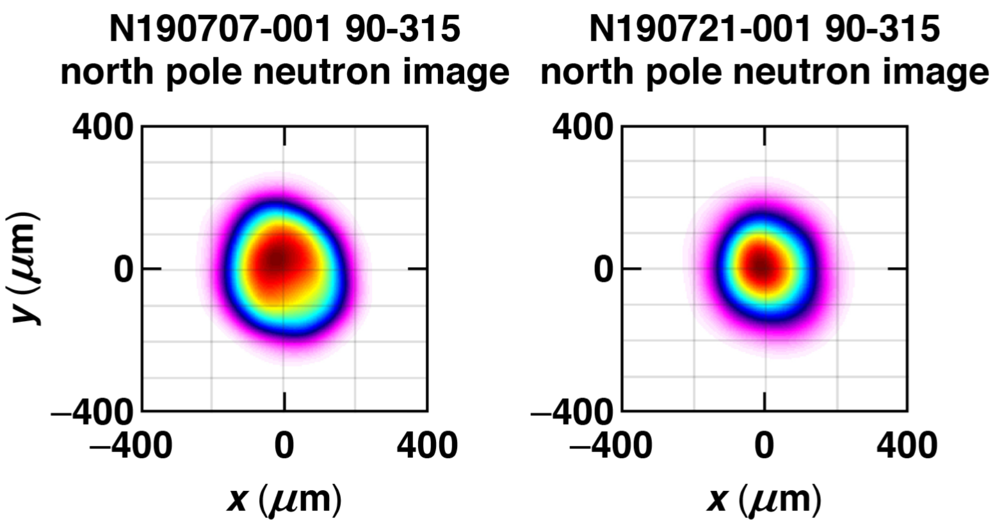

TC15253

- Future shots will strive to correct the oblate equatorial neutron morphology using pointing and pulse shapes
- Increasing peak power increases yield
- A systematic scan of fill pressure and peak power at this low laser impact will help steer designs before attempting larger targets

* Yeamans, Kemp; Lawrence Livermore National Laboratory, private communication (2019).

** P. Volegov, Los Alamos National Laboratory, private communication (2019).

Exploding pusher (XP) designs using *DRACO* with pump depletion provide a pathway to higher yields while forming a platform to study laser-energy coupling

UR LLE

- **Recent NIF XP shots in polar direct drive (PDD) induce unbounded cross-beam energy (CBET) gain given the infinite source-term of the Randall formulation***
- **Pump depletion naturally limits CBET gain by reducing the pump-field magnitude and converges to a physically realistic solution without *ad hoc* multipliers**
  - **applicable to both low- and high-intensity implosions****
- **The CBET modeling with pump depletion facilitates predictive simulations**

* C. J. Randall, J. R. Albritton, and J. J. Thomson, Phys. Fluids 24, 1474 (1981).
** P. W. McKenty *et al.*, YO6.00006, this conference.
K. Anderson *et al.*, NO5.00009, this conference.
NIF: National Ignition Facility

<BackUp slides …>

17

words

18

The ASR within a computational-cell tends to be star-shaped when accumulating the contributions from every beam

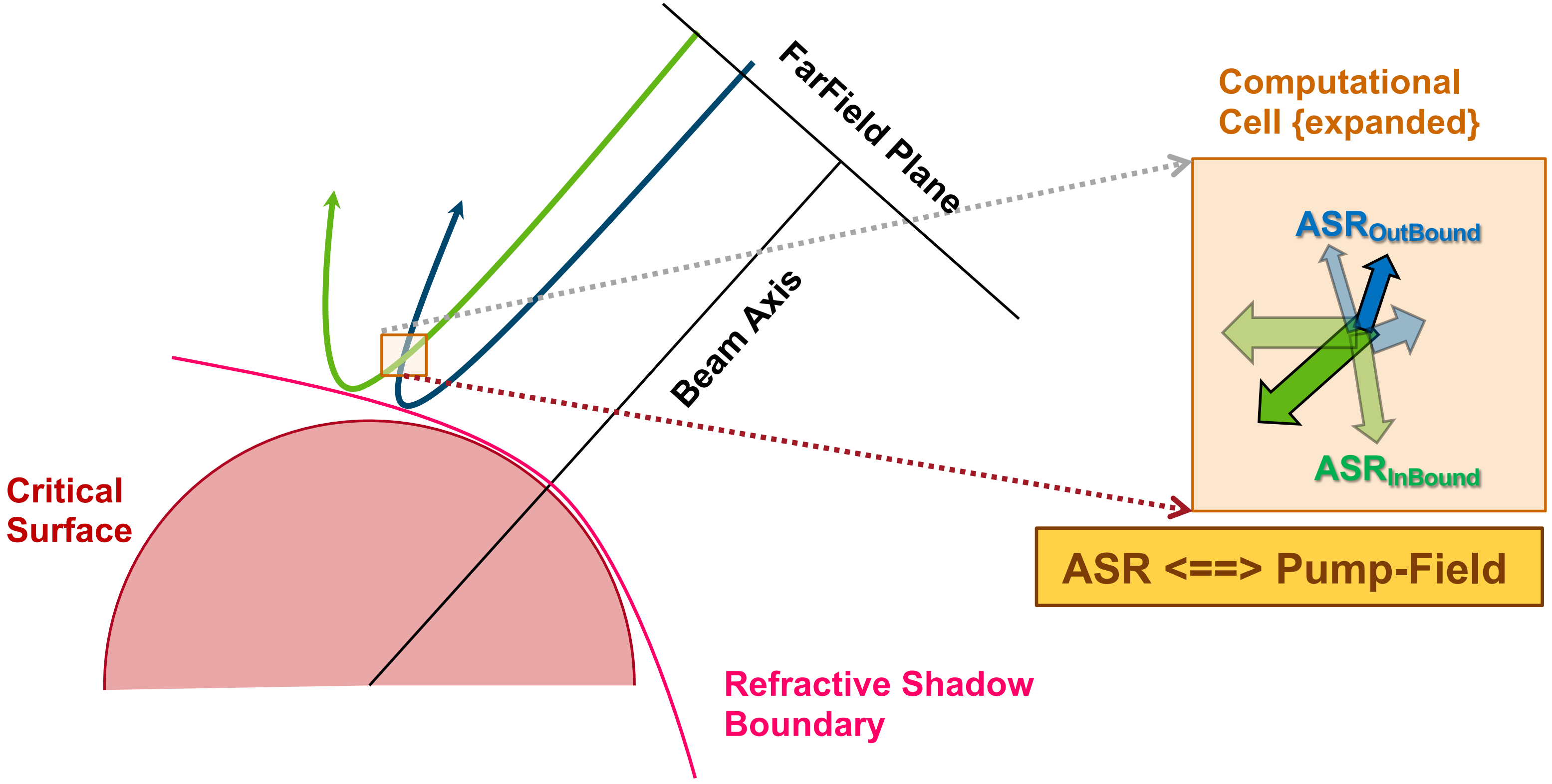

- The ASR pump-spectrum peaks in a direction corresponding to each beam
  - Single cell can include both in-bound and out-bound dominant directions for each beam
- When all contributing beams are included the ASR object becomes star-shaped
- The lobe width, direction and strength depends on the location in the plasma
  - Each lobe can be emulated with a $\{1,3,5,9\} \in$ N-point stencil in a k-local model

A post-shot simulation of N190227 models the relevant physics and closely predicts the experimental DT-yield (1.1e16)

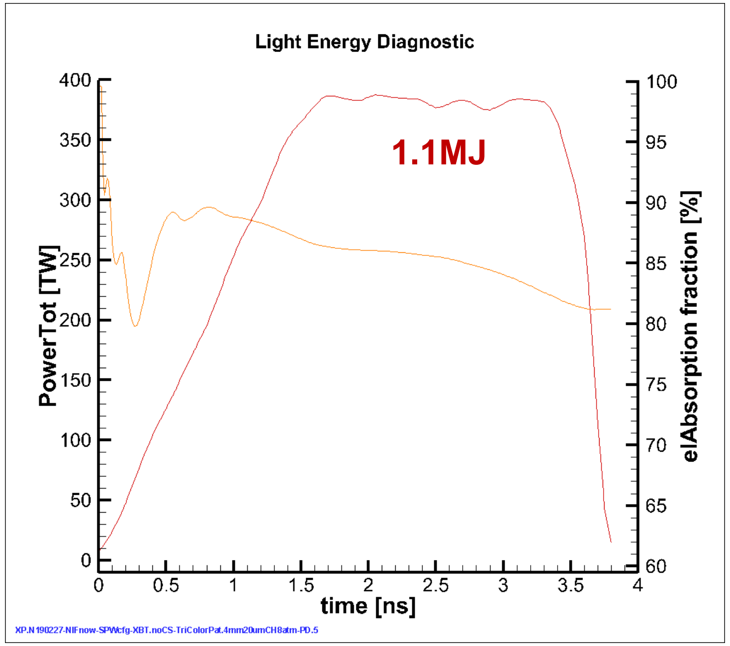

N190227 4mm,25um-CH 8atm-DT (65/35), $\Delta\lambda_0 = \{9.7, 8.5, 1.2\}$Å, IR

Draco:

Y_{DT} = 1.12e16
T_{ion} = 9.65 keV
t_{bang} = 4.25 ns
t_{width} = 300 ps

Exp:

Y_{DT} = 1.11e16
T_{ion} = 8.94 keV
t_{bang} = 4.22 ns
t_{width} = 452 ps

Simulation employed CBET w/ Pump-Depletion no-prefactors

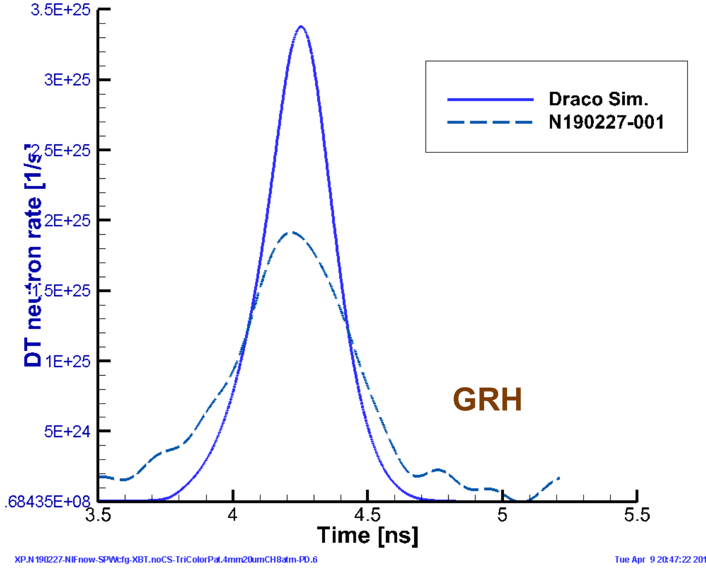

Laser-energy coupling loss caused by CBET can be mitigated in different domains that can be combined

- Spatial domain (reduction of the interaction volume)
  - dynamic spot-shape changes; "zooming"
    - reduces on-target energy, induces long-wavelength nonuniformity, and increases imprint
  - spot-shape apodization
    - static spot-shape design tailored to the target
    - use optimal super-Gaussian shape while not altering imprint
- Spectral domain (wavelength detuning)
  - detuning shifts resonances into lower interaction volumes
  - does not induce spot-shape distortion or imprint
  - all required technologies exist, i.e., no R&D; low risk
  - will cause system-wide optics upgrades and downtime; high cost
  - detuning is more effective in PDD
- Temporal domain
  - time multiplexed pulses reduce interaction-time overlap
  - requires short pulses to minimize affect on hydrodynamics
  - causes increased peak power

TC12956

The interaction of crossed laser beams within an expanding plasma causes CBET between beams

- This stimulated Brillouin scattering (SBS)-based interaction leads to a resonance condition for transferring energy between a pump ray and a probe ray by means of an ion-acoustic wave k_a*

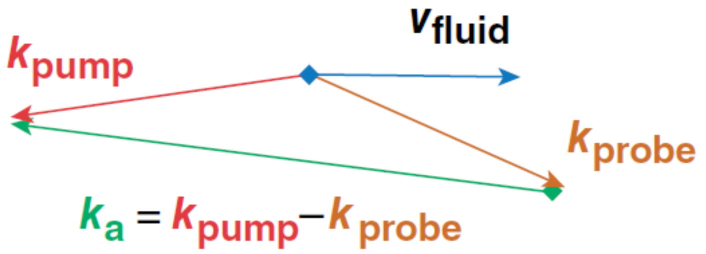

- The resonance condition peaks when the matching condition is met

$$\eta = \frac{(\omega_{\text{pump}} - \omega_{\text{probe}}) - k_a \cdot v_{\text{fluid}}}{|k_a| c_a} \qquad \begin{cases} \eta > 0; \text{gain} \\ \eta < 0; \text{loss} \end{cases}$$

*C. J. Randall, J. R. Albritton, and J. J. Thomson, Phys. Fluids 24, 1474 (1981).

The CBET effect is modeled by generalizing collinear interacting plane waves to include arbitrary incidence angles and polarization*

- The exponential CBET gain or loss factor is given by

$$d\tau_{XBT} = \zeta_{pol}\left[\frac{e^2}{c^3 m_e}\,\frac{n'_e}{1-n'_e}\,\frac{\lambda_0\langle Z\rangle}{\langle Z\rangle T_e + 3T_i}\right]\underbrace{P(\eta)\,I_{pump}}_{\text{ASR}}\,ds$$

$$P(\eta) = \frac{\eta\nu_a}{(\eta\nu_a)^2 + (1-\eta^2)^2}$$

Resonance function; **
$P = \pm 1/\nu_a$, when matched; i.e., $\eta = \pm 1$

$$\eta = \frac{(\omega_{pump} - \omega_{probe}) - k_a \cdot v_{fluid}}{|k_a| c_a}$$

Matching condition
$\begin{cases} \eta > 0;\ \text{gain} \\ \eta < 0;\ \text{loss} \end{cases}$

- Random polarization ζ_{pol} is included using either a constant 1/2 factor or $1/4\left\{1+\left[\hat{k}_{pump}\cdot\hat{k}_{probe}\right]^2\right\}$***
- Probe energy is gained or lost as $E_0\left[e^{d\tau_{IBS^\dagger}}\,e^{d\tau_{CBET}} - 1\right]$ in a cell

*C. J. Randall, J. R. Albritton, and J. J. Thomson, Phys. Fluids 24, 1474 (1981).
**ASR = angular-spectrum representation
***P. Michel, LLE/LLNL Meeting (May 2014).
†IBS = inverse bremsstrahlung

TC11307b

The CBET interactions can be grouped roughly into two modes

- The laser-beam interaction for directly driven targets (symmetric or PDD) covers a wide variety of angles, frequencies, and directions
  - refraction, chirping, and multibeam geometry are responsible

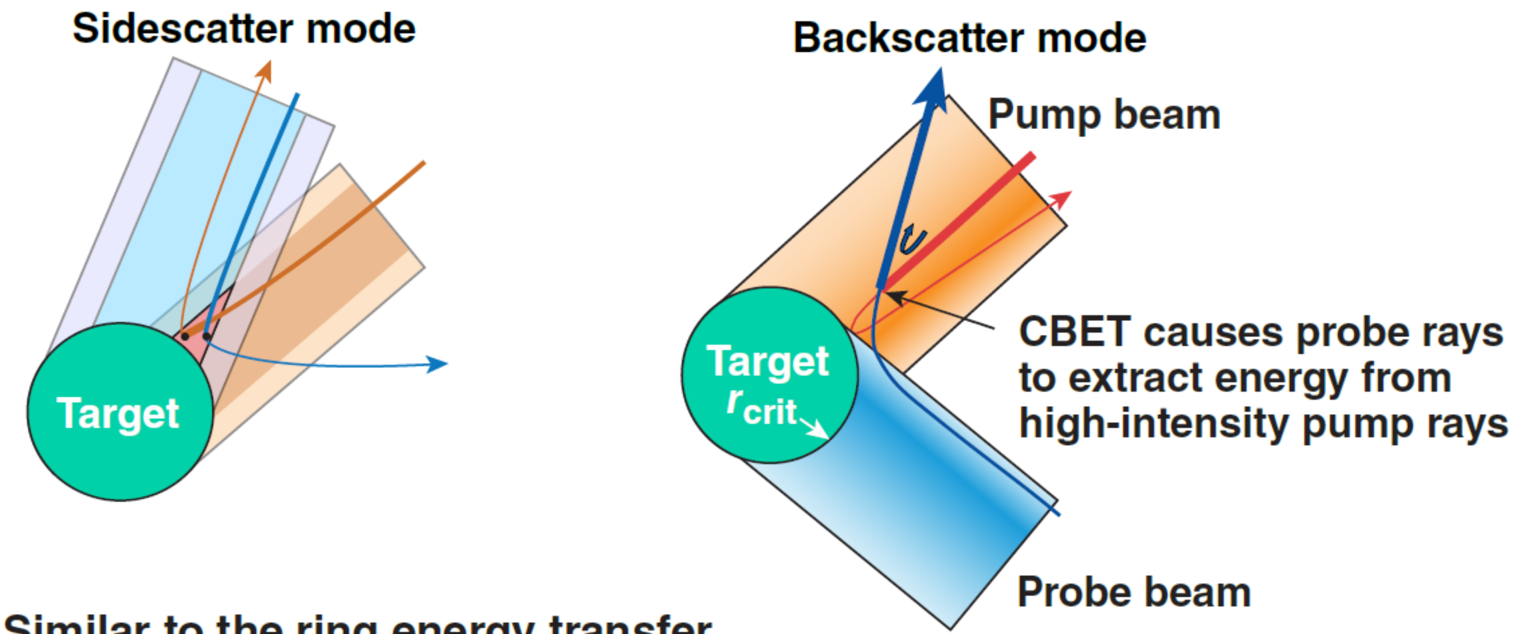

- Similar to the ring energy transfer used for NIF indirect-drive ignition (IDI)
- Has minimal impact on absorption

- The primary CBET mode that reduces energy absorption

TC11305e

The sidescatter mode causes an inbound beam-to-beam CBET exchange

- The sidescatter mode occurs when both beams are inbound or outbound

Sidescatter mode

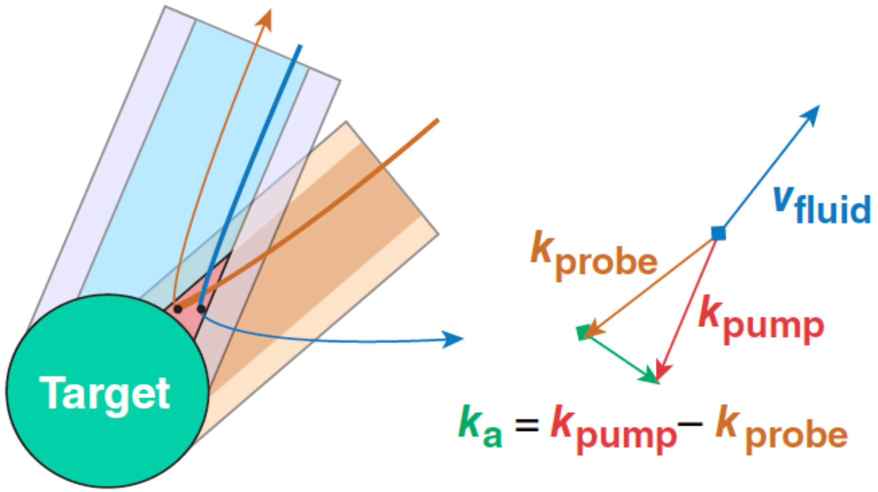

Matching condition

$$\Delta\omega = \omega_{pump} - \omega_{probe} = |k_a| c_a + k_a \cdot V_{fluid}$$

$$\lim_{V_{fluid} \to M c_a \hat{r}} \Rightarrow \eta = \frac{\Delta\omega - |k_a| c_a M \cos\theta_{k_a}}{|k_a| c_a}$$

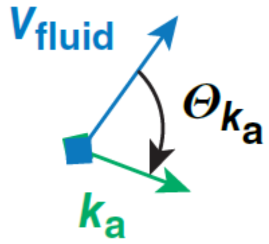

- The resonance condition still peaks where the fluid is supersonic (small $\Delta\omega$)
- The $|k_a|$ is much smaller, however, and the angle θ_{k_a} can be near orthogonal, which implies that the $k_a \cdot V_{fluid}$ term no longer dominates
  - the sign of the $\Delta\omega$ can now determine gain/loss for smaller values

TC11309b

The backscatter-mode dominates CBET-losses for directly-driven targets

- **The backscatter mode occurs for opposing beams**

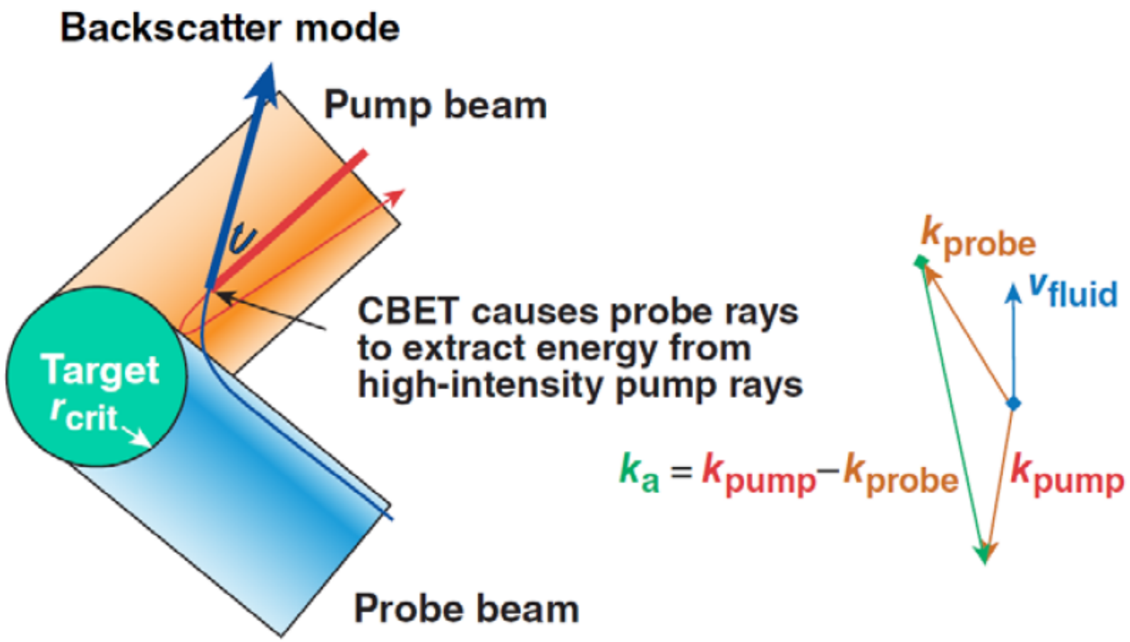

Omega experiment and simulation

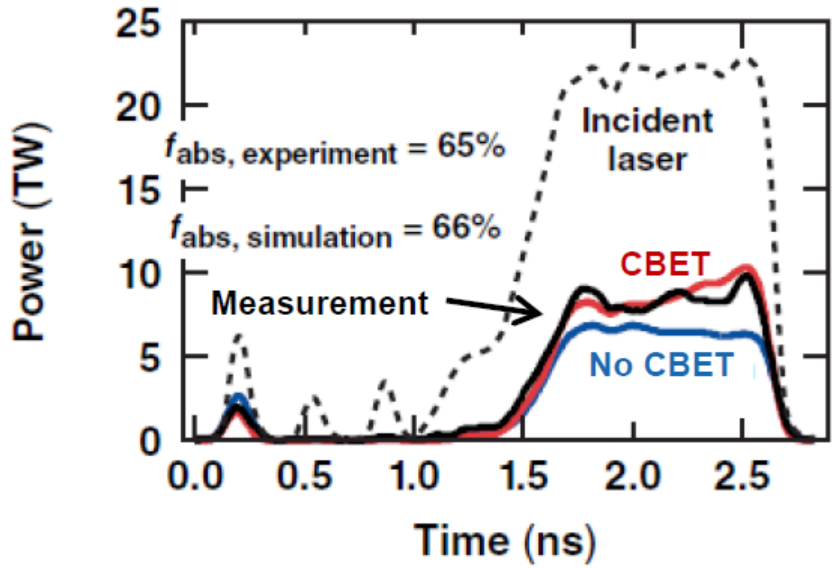

- **The outbound ray in backscatter mode always gains energy regardless of color ($\Delta\lambda_0 < |\pm 20\text{Å}, UV|$)**
- **Leads to deposition nonuniformity; mitigation can correct**

- **One of many measurements constraining simulations to include CBET**

<src TC11765e >

The backscatter mode dominates the CBET loss for directly driven targets

- The backscatter mode occurs for opposing beams

Backscatter mode

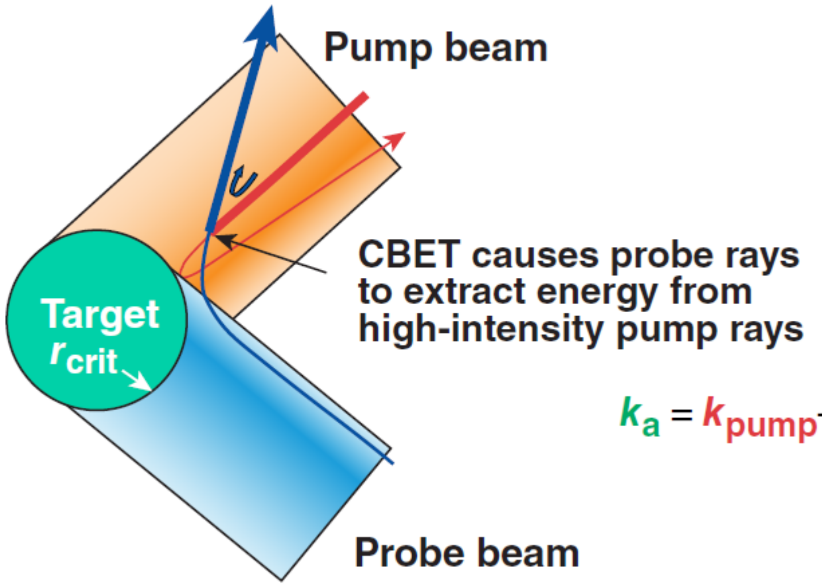

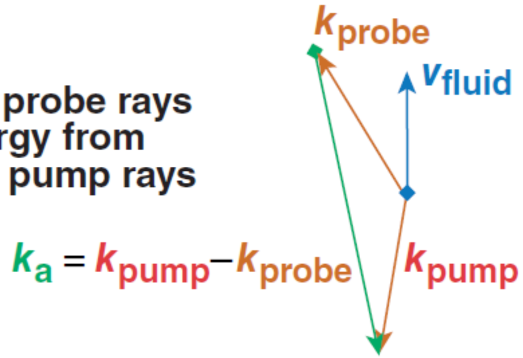

Matching condition

$$\Delta\omega = \omega_{pump} - \omega_{probe} = |k_a| c_a + k_a \cdot V_{fluid}$$

$$\lim_{V_{fluid} \to M c_a \hat{r}} \Rightarrow \eta = \frac{\Delta\omega - |k_a| c_a M\cos\theta_{k_a}}{|k_a| c_a}$$

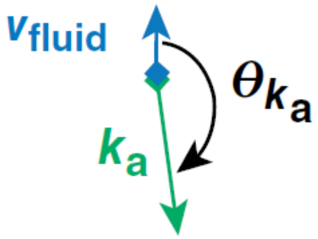

- The resonance condition peaks where the fluid is supersonic (small $\Delta\omega$)
- As the frequency difference increases, the resonance condition shifts to lower/higher sonic speeds depending on the sign (e.g., $M = \{0.4, 1.6\}$ for ±6-Å UV)
  - dominated by the $k_a \cdot V_{fluid}$ term; its sign determines whether there is gain/loss
  - frequency difference cannot alter the gain/loss unless it can counter the large $k_a \cdot V_{fluid}$ term (e.g., ±20-Å UV)

Successful wavelength detuning shifts the resonance location sufficiently to mitigate CBET

When probe rays are blue-shifted, the resonance shifts to a higher Mach number where intersecting probe rays are negligible

When probe rays are red-shifted, the resonance shifts to a lower Mach number where probe rays are blocked and/or have negligible intensity

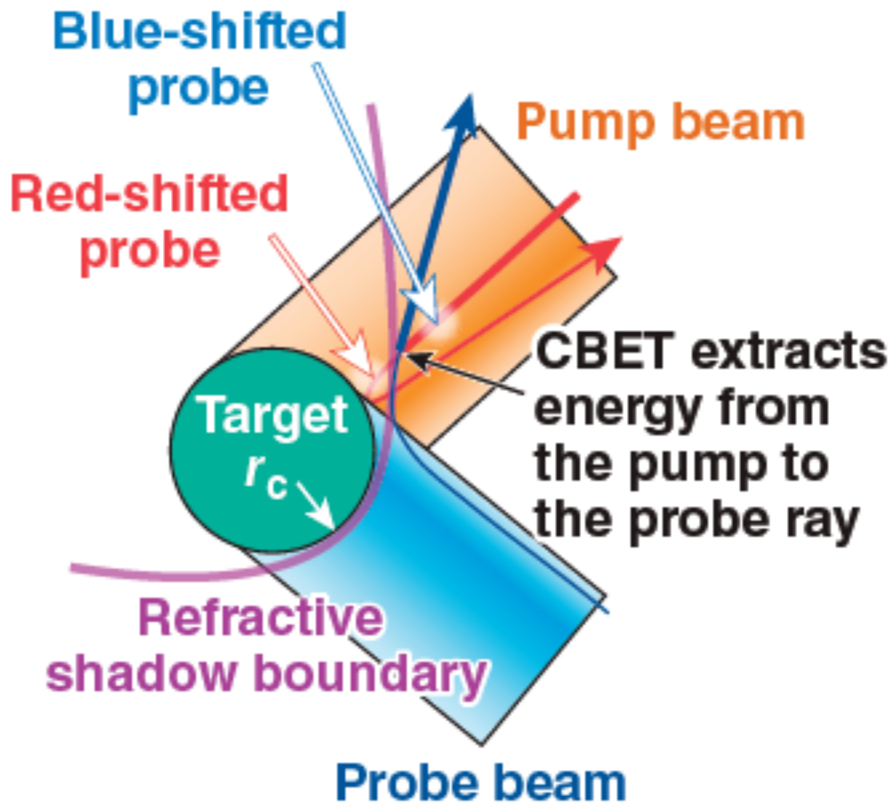

- The magnitude of $\Delta\lambda_0$ determines the mitigation duration
  - works for both symmetric and PDD
  - tailoring the spot shape will help limit the required $\Delta\lambda_0$

TC11766f

Four main categories of reducing laser deposition noise are included in the LLE [1] raytrace; staged approach

- Raytrace noise reduction
  - An inverse-projection algorithm defines the initial ray-positions distribution and energies -- Complete
    - This is the primary noise reduction feature
  - Dynamic adjustment of inverse-projection partially compensates for refraction and reduces noise
    - In progress
  - Adaptive integrators
    - Future work
  - Accurate cell-edge crossing detection using root-polishing; never loses a ray on entry/exit
    - Future work

Phase-1

Phase-2

Phase-3

Phase-4

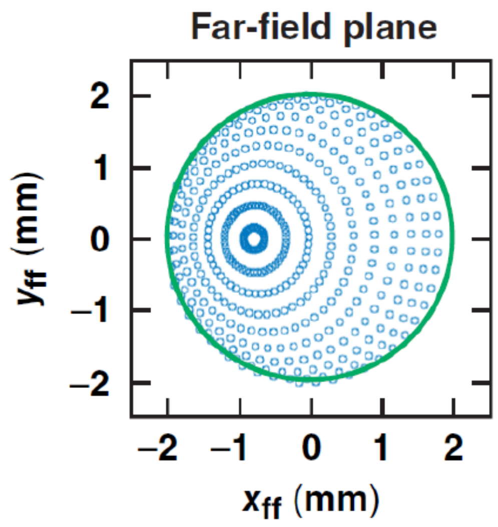

Inverse Projection

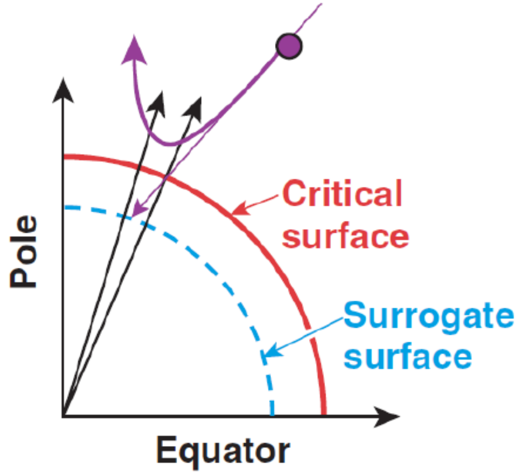

Refraction Compensation

[1] J.A. Marozas, et al., PoP (2018)

Phase-1

The basic inverse projection algorithm maps-out the %-critical surfaces to form a set of aim-points in 3-D Hydra

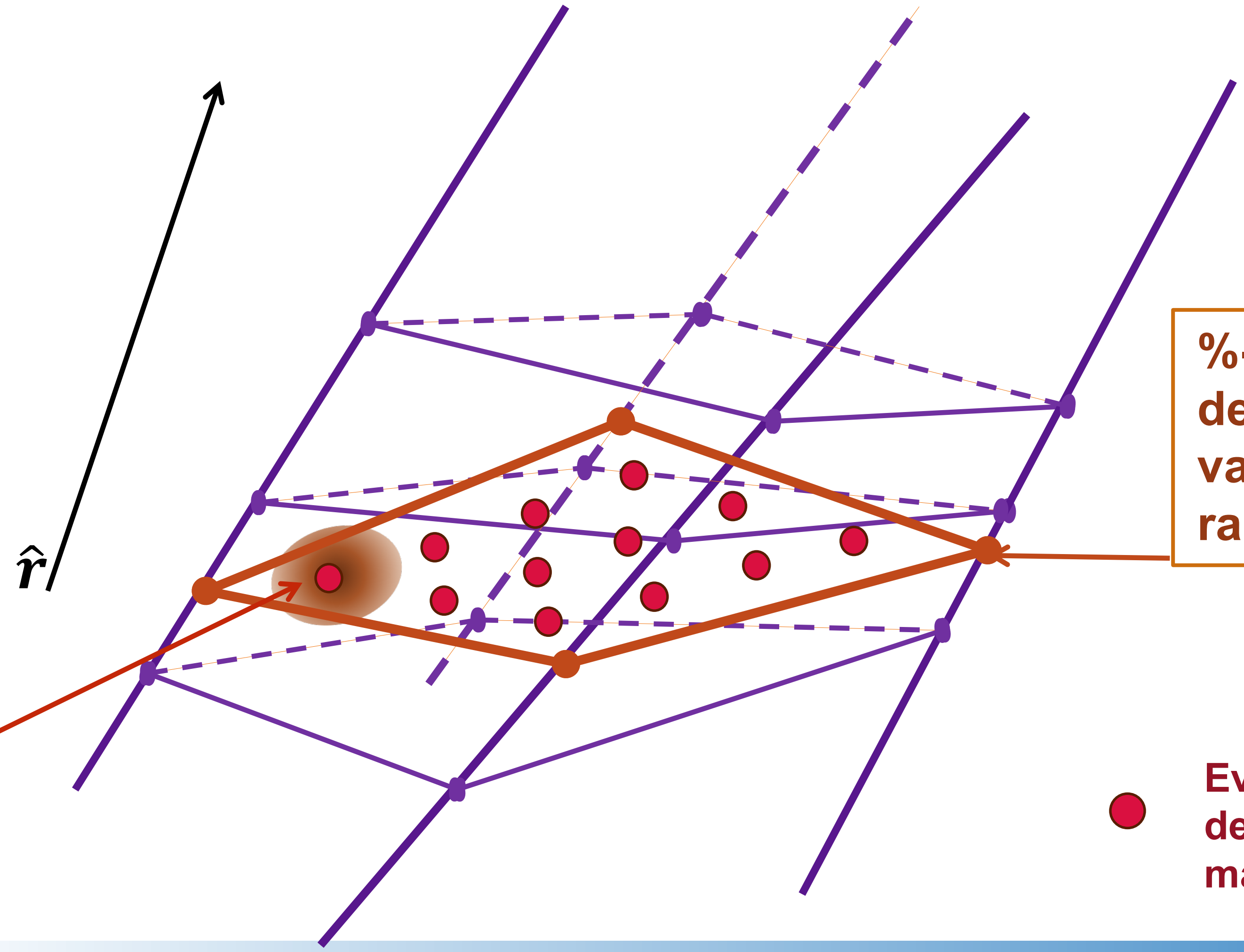

%-Critical surface defined by interpolated values along Hydra's radial logical-coordinate

Supports aim-point random dithering
- Which further reduces noise

Aim-Points

Evenly distributed interior points described using an isoparametric mapping of the %-Critical surface

Phase-1

The basic inverse projection algorithm back-projects the aim-point distribution onto the far-field plane to form the set of launch-points that do not bias the modal pattern

Rays are aimed at evenly distributed points using an isoparametric mapping within Hydra's cells

In the far-field plane, the back-projected points sample the intensity and derive energy from their area projections

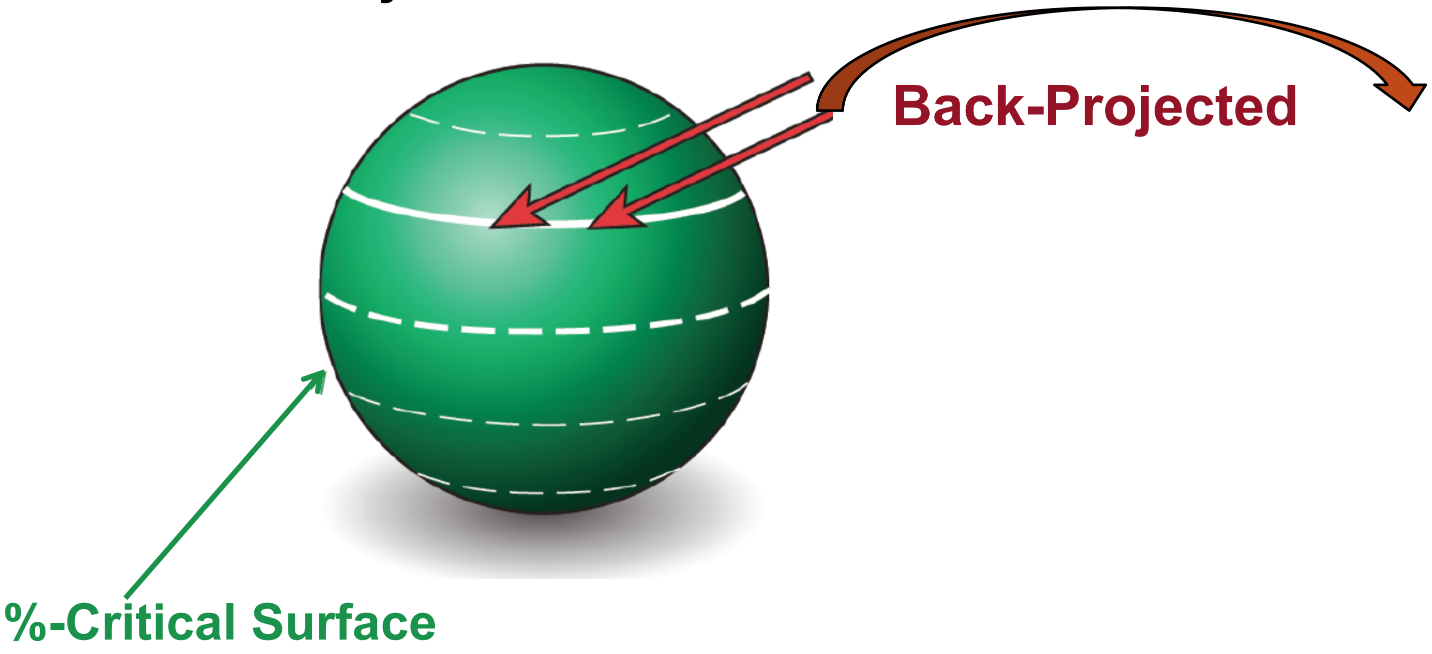

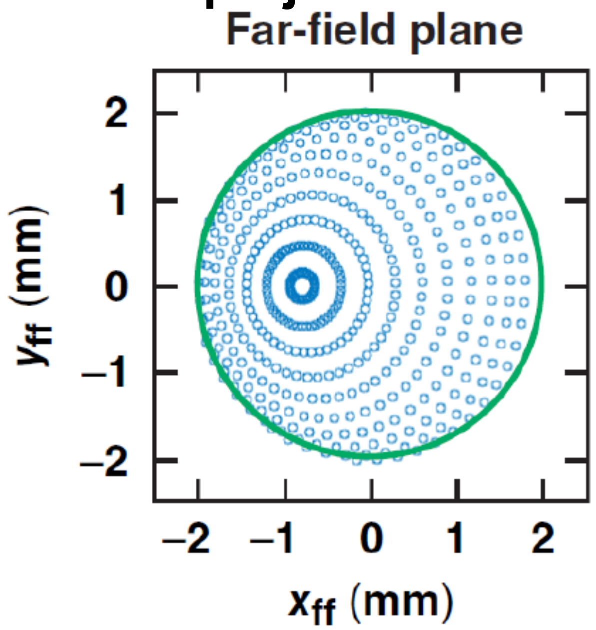

- **Once the atmosphere develops, many layers of %-critical form the surfaces**